Sphingosine 1-Phosphate Receptor 5 (S1P5) deficiency promotes proliferation and immortalization of Mouse Embryonic Fibroblasts

Franck Talmont, Elodie Mitri, Christine Dozier, Arnaud Besson, Olivier Cuvillier, Anastassia Hatzoglou

▶ **To cite this version:**

Franck Talmont, Elodie Mitri, Christine Dozier, Arnaud Besson, Olivier Cuvillier, et al.. Sphingosine 1-Phosphate Receptor 5 (S1P5) deficiency promotes proliferation and immortalization of Mouse Embryonic Fibroblasts. 2022. hal-03808905v1

HAL Id: hal-03808905

https://cnrs.hal.science/hal-03808905v1

Preprint submitted on 14 Feb 2022 (v1), last revised 20 Jun 2023 (v2)

HAL is a multi-disciplinary open access archive for the deposit and dissemination of scientific research documents, whether they are published or not. The documents may come from teaching and research institutions in France or abroad, or from public or private research centers.

L'archive ouverte pluridisciplinaire **HAL**, est destinée au dépôt et à la diffusion de documents scientifiques de niveau recherche, publiés ou non, émanant des établissements d'enseignement et de recherche français ou étrangers, des laboratoires publics ou privés.

Sphingosine 1-Phosphate Receptor 5 (S1P5) deficiency promotes proliferation and immortalization of Mouse Embryonic Fibroblasts

Franck Talmont [1,*], Elodie Mitri [2,*], Christine Dozier [2], Arnaud Besson [2], Olivier Cuvillier [1,‡], Anastassia Hatzoglou [1,2,‡]

[1] Institut de Pharmacologie et de Biologie Structurale, Université de Toulouse, CNRS, UPS, Toulouse, France

[2] MCD, Centre de Biologie Intégrative, Université de Toulouse, CNRS, UPS, Toulouse, France

* These authors contributed equally to this work

‡ Corresponding authors

Tel: +33 5 61 17 58 42

Email: anastassia.hatzoglou-robbiola@univ-tlse3.fr; olivier.cuvillier@inserm.fr

Keywords: sphingosine-1phosphate, S1P5, MEF immortalization, cell proliferation, cell spreading, cell migration, ERK, FAK

ABSTRACT

Sphingosine 1-phosphate (S1P), a bioactive lipid, interacts with five widely expressed G protein-coupled receptors (S1P1-5), regulating a variety of downstream signaling pathways with overlapping but also opposing functions. To date, data regarding the role of S1P5 in cell proliferation are ambiguous, and its role in controlling the growth of untransformed cells remains to be fully elucidated. In this study, we examined the effects of S1P5 deficiency on mouse embryonic fibroblasts (MEFs). Our results indicate that lack of S1P5 expression profoundly affects cell morphology and proliferation. First, S1P5 deficiency reduces cellular senescence and promotes MEF immortalization. Second, it decreases cell size and leads to cell elongation, which is accompanied by decreased cell spreading and migration. Third, it increases proliferation rate, a phenotype rescued by the reintroduction of exogenous S1P5. Mechanistically, the anti-proliferative function of the S1P/S1P5 axis is associated with reduction in nuclear accumulation of activated ERK. Our results suggest that S1P5 opposes the growth-promoting function of S1P1-4 through spatial control of ERK activation and provide new insights into the anti-proliferative function of S1P5.

INTRODUCTION

Sphingosine 1-phosphate (S1P) is a pleiotropic bioactive lipid found in organisms as diverse as yeast, flies, plants and mammals, which has been implicated in a variety of cellular responses including cell growth and migration [1-3]. S1P exerts intracellular functions or acts extracellularly in an autocrine or paracrine manner through a family of five specific G-protein-coupled receptors (S1PRs), called S1P1-5, in an autocrine or paracrine manner [4]. Extracellular S1P signaling depends on which receptor subtypes are expressed [5], as S1P1-5 couple to different G proteins, and thus regulate various downstream signaling pathways with overlapping but also opposing functions [6].

Deregulation of sphingolipid metabolism, such as altered S1P levels and/or expression/activation of S1P receptors, has been linked to a variety of pathological conditions, including cancer, diabetes, fibrosis, inflammatory disorders, and multiple sclerosis [7,8]. Thus, S1P receptors contribute to tissue homeostasis and constitute challenging therapeutic targets. For example, FTY720 (Fingolimod), a sphingosine analog, which binds with similar affinities to S1P1 and S1P5, was approved by the US Food and Drug Administration (FDA) in 2010 for the treatment of relapsing-remitting multiple sclerosis [9]. It can be phosphorylated *in vivo* to form FTY720-phosphate (FTY720-P), an S1P mimetic interacting with S1P receptors but preferentially inducing internalization and degradation of S1P1 [10]. While the cellular functions of S1P1 and its internalization upon binding to S1P have been well studied, little is known about the roles of S1P5 and the underlying molecular mechanisms. Data on cellular functions of S1P5 are indeed scarce and contradictory. A limited number of studies have examined the role of S1P5 in brain and natural killer cells, where S1P5 is highly expressed. S1P5 has been involved in oligodendrocyte survival and maintenance of blood-brain barrier integrity, while in natural killer cells it controls egression to the lymphatic system [11-13]. S1P5 may also mediate S1P-induced autophagy in breast cancer cells [14], while S1P5 overexpression is associated with decreased proliferation of esophageal cancer cells [15]. We recently reported that S1P regulates proper mitotic progression in various cell types through the S1P5/AKT/PLK1 pathway [16,17].

In this study, we investigated the consequences of S1P5 loss in primary and immortalized mouse embryonic fibroblasts (MEF). S1P5 deficiency reduces cellular senescence and promotes primary MEF immortalization. Our results suggest that S1P/S1P5 signaling decreases cell growth and opposes the growth-promoting functions of S1P/S1P1-3 through the spatial control of ERK activation, providing new insight into the anti-proliferative function of S1P5.

RESULTS

S1P5 deficiency confers resistance to cellular senescence and promotes MEF immortalization

To investigate the effect of S1P5 loss on MEF proliferation, freshly isolated MEFs from S1P5 wild-type ($S1P5^{+/+}$) and S1P5 deficient ($S1P5^{-/-}$) mice were cultured using the 3T3 protocol [18]. Cells were seeded at $3x10^5$ in 10 cm dishes and re-plated twice a week to prevent MEFs from reaching contact inhibition. As expected, primary MEFs exit the cell cycle as the number of passages increases, resulting in a growth arrest phase on average at passage 6-7 (Figure 1A) [18]. However, $S1P5^{-/-}$ MEFs resumed proliferating after a short growth stasis (passage 7 to 9), indicating the emergence of immortalized clones [19] (clone $S1P5^{-/-}$ 3 was lost at passage 15 after contamination). The growth of wild-type MEFs decreased over time and only one out of the three starting lines eventually became immortalized at passage 16 (Figure 1A). Consistent with these observations, $S1P5^{-/-}$ MEFs exhibited higher BrdU incorporation at passages 6 and 12 compared to wild-type $S1P5^{+/+}$ MEFs (Figure1B). In addition, clonogenicity assays showed that S1P5-deficient cells at low passage formed more colonies than wild-type cells (Figure 1C). These results suggest that S1P5 deficiency might protect cells from cellular senescence. Indeed, loss of S1P5 significantly reduced the percentage of SA-β-gal-positive cells compared to wild-type MEFs, however, despite their ability to grow, some $S1P5^{-/-}$ cells retained some features of cell senescence such as β-gal staining (Figure 1D) [20]. Taken together, these results indicate that S1P5-deficiency promotes MEF immortalization and protects them from cellular senescence.

S1P5 loss results in cell elongation and impaired adhesion, spreading and migration

S1P5 deficiency causes changes in cell morphology. $S1P5^{-/-}$ cells were more refractile and exhibit decreased in size compared to wild-type MEFs (Figure 2A, left panel). Loss of S1P5 expression resulted in cell elongation, which was quantified by measuring the ratio of their maximal length to width, compared with wild-type MEFs (Figure 2A, right panel). Furthermore, cell surface area was significantly reduced in $S1P5^{-/-}$ cells compared to wild-type MEFs (Figure 2B). In association with these morphological changes, phalloidin staining revealed changes in F-actin distribution, with pronounced cortical actin in

S1P5$^{-/-}$ cells (Figure S1A). In addition, vinculin staining showed that there were fewer focal adhesion sites in S1P5$^{-/-}$ MEFs in agreement with their reduced size (Figure S1B).

Next, we compared the adhesion properties of S1P5$^{+/+}$ and S1P5$^{-/-}$ cells on glass coverslips coated or not with fibronectin at 0.5, 1 and 2 h after plating. At 1 and 2 h after plating, the number of S1P5$^{-/-}$ cells adhering to uncoated or fibronectin-coated coverslips was significantly reduced compared to wild-type MEFs (Figure 3A, B, respectively). After adhering to extracellular matrix (ECM), the cells spread out and acquire a flattened morphology [21]. As expected, wild-type MEFs spread isotropically, whereas S1P5$^{-/-}$ cells spread anisotropically, with membrane protrusions appearing within 30 min (Figure 3C, upper panel). Cell boundaries were visualized by phalloidin staining and quantification of the cell spreading was obtained by measuring the cell surface area. At all times studied, S1P5$^{-/-}$ cells spread significantly less than wild-type MEFs and at 3 h, the cell area of S1P5$^{-/-}$ cells was reduced by 75% of that of S1P5$^{+/+}$ MEFs (Figure 3C; 5157 ± 237 μm^2 versus 1777 ± 110 μm^2). Because cell spreading can affect cell migration, MEF motility was assessed by transwell assays. As shown in Figure 3D, loss of S1P5 expression significantly inhibited MEF cell migration.

Focal adhesion kinase (FAK) plays a crucial role in transducing signals initiated by the interaction between integrins and ECM proteins, which in turn regulate cell adhesion, spreading and migration [22]. The impaired spreading and migration of S1P5$^{-/-}$ MEFs raised the possibility of a role of S1P5 in FAK activation. When serum-starved wild-type cells were stimulated with S1P, FAK was rapidly phosphorylated and activation lasted for at least 30 min (Figure 3E). In contrast, S1P5$^{-/-}$ cells did not activate FAK upon S1P treatment, suggesting that S1P induces FAK activation via S1P5 (Figure 3E). Interestingly, under basal culture conditions (24 h in 10% FBS-containing medium), FAK phosphorylation is reduced in S1P5$^{-/-}$ MEFs compared to wild-type S1P5$^{+/+}$ cells (Figures 3E and S2), confirming that S1P5 is required for FAK phosphorylation induced by mitogenic factors in FBS. Taken together, these results indicate that the S1P/S1P5 signaling pathway promotes FAK activation and is required for downstream cell spreading and motility.

Loss of S1P5 promotes cell proliferation

The proliferation of immortalized S1P5$^{+/+}$ and S1P5$^{-/-}$ MEFs (passages 18-22) was assessed by counting cells by trypan blue staining. As shown in Figure 4A, S1P5$^{-/-}$ MEFs showed a growth advantage compared to wild-type cells over a 4-day period. In agreement with the literature, the average cell cycle length for wild-type MEF was 24 h, whereas it was approximately 18 hours in S1P5$^{-/-}$ MEFs. Furthermore, S1P5$^{-/-}$ cells had a survival advantage over wild-type cells, as shown by MTT (Figure 4B) and colony formation assays (Figure 4C), although there was no significant difference in cell death monitored by trypan blue staining (Figure 4D). During this work, a second wild-type S1P5$^{+/+}$ immortalized line (S1P5$^{+/+}$2) was generated in the laboratory and had similar proliferation characteristics as the first one. Both wild-type clones proliferated slower than S1P5$^{-/-}$ cells (Figure 4E). Overall, these results suggest that immortalized S1P5$^{-/-}$ MEFs proliferate more rapidly than S1P5$^{+/+}$ cells.

To confirm the role of S1P5 in regulating cell proliferation, S1P5 was reintroduced in S1P5$^{-/-}$ MEFs. Because we were unable to obtain MEFs stably expressing S1P5, growth properties were assessed in cells transiently expressing mouse S1P5 fused to GFP (mS1P5-GFP). Expression of mS1P5-GFP in S1P5$^{-/-}$ cells at least partially reduced proliferation compared to control GFP transfected cells (Figure 4F). However, this partial effect could be due to the low transfection rate (30-40%) and the fact that un-transfected cells continued to proliferate at an increased rate and rapidly dominated the cultures. Since both S1P5$^{-/-}$ clones show similar growth properties, clone 2, designated S1P5$^{-/-}$, was used for further study. In conclusion, these results strongly suggest that the S1P5 receptor inhibits cell proliferation.

We have previously shown that MEFs express all S1P receptors [16], which makes it difficult to study the specific functions of S1P5. In contrast, CHO cells do not express any S1P receptors and thus are a suitable model to dissect the cellular effects of single S1P receptors [23,24]. To define how S1P5 controls proliferation, CHO cells stably expressing either mS1P5-GFP or GFP as a control were generated (Figure 5A). S1P5-GFP exhibit a punctate localization in the cytoplasm and plasma membrane, whereas GFP is diffusely present in the nucleus and cytoplasm, as expected (Figure 5A). To verify that GFP-coupled S1P5 is functional, the ability of mS1P5-GFP to bind to a specific agonist (FTY720-P) was measured (EC50 = 3.01 +/- 1.12 nM), whereas no binding was observed in control GFP cells (Figure 5B).

In cell proliferation assays, cells expressing mS1P5-GFP showed considerably reduced cell numbers over 4 days compared with GFP control cells, confirming that S1P5 has an anti-proliferative activity when overexpressed in CHO cells (Figure 5C).

S1P5 decreases cell proliferation in an S1P/ligand dependent manner

We next investigated the molecular mechanism underlying S1P5-mediated cell growth inhibition. Indeed, S1P1-5 are activated by intracellular and extracellular S1P but may also have ligand-independent roles. The decrease in cell number in mS1P5-GFP compared to GFP cells was not due to the apoptosis since experiments performed in presence of the pan-caspase inhibitor Z-VAD gave similar results (Figure 6A). FTY720-P is a potent S1P receptor ligand that induces internalization, sequestration or degradation of S1P receptors, thus acting as an inhibitor when present for long periods of time [10]. S1P5-induced inhibition of proliferation was rescued when cells were grown in the presence of FTY720-P (Figure 6A). Because S1P is present in the serum [25], we used Sphingomab, a high-affinity anti-S1P (αS1P) monoclonal antibody that neutralizes extracellular S1P [16,26]. Addition of αS1P to the culture medium specifically reversed the S1P5-induced growth phenotype compared to control antibodies, indicating that extracellular S1P inhibits CHO cell growth via activation of S1P5 (Figure 6B). Furthermore, control (GFP) and S1P5 (mS1P5-GFP) expressing cells grown in media containing delipidated charcoal-stripped FBS (csFBS) had similar growth properties, confirming that S1P present in the serum is required for S1P5-induced growth inhibition. Addition of exogenous S1P restored the inhibition of proliferation of S1P5-expressing cells cultured in csFBS, and this effect was prevented by neutralizing αS1P (Figure 6C). Taken together, these results indicate that S1P/ S1P5 signaling results in growth inhibition.

The S1P/S1P5 axis negatively regulates MEF proliferation

Because all S1PRs are expressed in MEFs [16], we studied the involvement of the S1P/S1P5 axis in MEF proliferation in the context of the presence of all the other S1PRs. As in CHO cells, the cell growth advantage induced by loss of S1P5 was independent of apoptosis since Z-VAD had no effect (Figure 7A).

When cells were grown in presence of the S1P1-5 functional antagonist FTY720-P, wild-type and $S1P5^{-/-}$ cells showed similar proliferation rates. Importantly, FTY720-P significantly reduced the number of $S1P5^{+/+}$ cells compared to untreated cells (DMSO), suggesting that S1P1-4 receptors positively regulate MEF proliferation (Figure 7A). To examine the involvement of S1P1-3 receptors in MEF proliferation, these assays were performed in presence of the pharmacological inhibitors VPC23019 (specific for S1P1 and S1P3) and JTE-013 (specific for S1P2). Inhibition of S1P1-3 significantly decreased cell growth in wild-type cells compared to untreated cells (69% vs 100%; Figure 7A) suggesting that one or more S1P1-3 receptors promote cell proliferation in immortalized MEF. In contrast, in the presence of VPC23019 and JTE-013, $S1P5^{-/-}$ cells continued to proliferate significantly faster than $S1P5^{+/+}$ cells, further confirming that S1P5 has an anti-proliferative effect.

We next investigated whether extracellular S1P controlled MEF cell growth via S1P5. When MEFss were grown in the absence of extracellular S1P (delipidated csFBS) or in presence of extracellular S1P neutralizing antibodies (αS1P), $S1P5^{+/+}$ and $S1P5^{-/-}$ cells had similar proliferation rates and the growth advantage of $S1P5^{-/-}$ cells was reversed (Figure 7B). Overall, these results strongly suggest that S1P inhibits MEF proliferation via S1P5.

Loss of S1P5 leads to persistent activation of ERK and its nuclear localization

Since the MAPK and Akt signaling are crucial to MEF proliferation, we studied the phosphorylation level of ERK and Akt under basal culture conditions. Akt phosphorylation was decreased in $S1P5^{-/-}$ cells cultured for 24 hours in medium supplemented with 10% FBS, whereas under the same culture conditions, ERK phosphorylation was increased in $S1P5^{-/-}$ cells compared with $S1P5^{+/+}$ MEFs, suggesting that S1P5 negatively regulates ERK activation by mitogenic factors present in FBS (Figure 8A). Phosphorylated ERK shuttles between the cytoplasm and the nucleus, and nuclear phospho-ERK has been shown to promote MEF proliferation while cytoplasmic phospho-ERK induces cell cycle arrest and growth inhibition [27]. As temporal but also spatial control of ERK activation is crucial for cell fate decisions, we investigated whether the increased ERK phosphorylation in S1P5-deficient cells correlates

with its nuclear localization. As seen in Figure 8B, phosphorylated ERK accumulated in the nuclei of $S1P5^{-/-}$ cells compared with proliferating $S1P5^{+/+}$ MEFs. Nuclear boundaries were defined by Hoechst 33342 staining and the phospho-ERK staining intensity per nuclei was quantified. The intensity of nuclear phosphorylated ERK was significantly elevated in S1P5-deficient cells compared with wild-type cells (Figure 8C; 603.6 ± 30.8 versus 423.3 ± 33.3 respectively). These results suggest that S1P5 downregulates FBS-induced activation of ERK, by controlling the spatiotemporal ERK phosphorylation resulting in decreased proliferation.

Discussion

The cellular functions of the S1P receptor S1P5 are still poorly characterized. It is well established that S1P5 affects immune quiescence of the brain endothelial barrier, as well as natural killer cell trafficking [12,13,28]. Other studies have shown that in cancer cells, S1P5 regulates mitotic progression and autophagy [16,29], and S1P5 overexpression inhibits the growth of esophageal squamous cell carcinoma Eca 109 cells [15]. Thus, the current knowledge regarding the effects of S1P5 on cell proliferation and migration is limited and still remains uncharacterized in untransformed cells. In this work, we investigated the effects of S1P5 deficiency in MEFs and showed that lack of S1P5 promotes immortalization and cell proliferation by controlling the spatiotemporal activation of ERK. We also find that, in $S1P^{-/-}$ MEFs, cell spreading, adhesion and migration are compromised and those phenotypes involve FAK activation.

S1P5 deficiency resulted in cell elongation and decreased cell surface area, while cell adhesion and spreading were compromised. The actin filament network and the focal adhesion sites (FA) are major regulators of cell spreading and morphology and initiate migration in various cell types, including fibroblasts [30]. MEF adhesion requires focal adhesion kinase (FAK), a highly conserved cytoplasmic enzyme, activated when integrins bind to ECM proteins, and in turn phosphorylated FAK activates several proteins including Rho GTPases involved in F-actin organization and dynamics [31,32]. Consistent with this model, $S1P5^{-/-}$ cells exhibited fewer and sparser focal adhesion sites and increased cortical actin. A similar phenotype has been reported for $FAK^{-/-}$ MEFs [33], supporting that FAK acts downstream of S1P/S1P5 to control cell adhesion and spreading. It has been reported that S1P rapidly induces FAK phosphorylation in endothelial cells, but the involvement of one or more specific S1P receptors is not clear [34-36]. Here we show for the first time that S1P-mediated FAK phosphorylation is mediated by S1P5 and that, in $S1P5^{-/-}$ cells, FAK activation is inhibited, which correlates with morphological changes and spreading defects. Finally, S1P5 positively regulated MEF migration. In agreement with our results, it was reported that Eca 109 esophageal cancer cells expressing GFP-S1P5 migrate faster than control cells under basal culture conditions [15]. Further studies are needed, including loss-of-function

strategies, to decipher the role of S1P5 in cancer cell migration and the role of actin regulators such as Rho GTPases downstream of S1P5.

Converging evidence suggests that S1P5 negatively regulates cell proliferation, but the underlying molecular mechanism remains unknown. Overexpression of S1P5 in Eca 109 (esophageal cancer cells) and CHO cells results in growth inhibition [15,24]. Here we show that primary and immortalized S1P5-deficient MEFs cells proliferate faster and form more colonies than wild-type cells, suggesting a tumor suppressor function for S1P5. Of note, S1P1-3 receptors promoted MEF proliferation while S1P/S1P5 signaling inhibited cell growth, suggesting that activation of a specific subset of receptors by S1P can induce different signaling pathways leading to opposite cell responses. In CHO cells overexpressing S1P5, S1P inhibits serum-induced phosphorylation of ERK [24] and the authors proposed that phosphatase PP2A acts downstream of the S1P/S1P5 pathway to limit ERK activation. ERK signaling plays a crucial role in various cellular functions such as cell proliferation, differentiation and survival. According to the current model, the spatiotemporal control of ERK activation (differences in duration and magnitude as well as in subcellular compartmentalization) would explain these distinct fates [27,37]. This spatiotemporal control of ERK activity is necessary for the control of MEF growth, with nuclear phospho-ERK leading to cell cycle progression, while the cytoplasmic phospho-ERK promotes cell cycle arrest [27,38]. Here we show that the absence of S1P5 results in sustained ERK activation when cells are grown in the presence of mitogenic factors and correlates with increased activated ERK in the nucleus. Activation of ERK by mitogenic factors is required for its nuclear translocation and nuclear activities [39], while its inactivation is mediated by the nuclear MAPK-specific phosphatases MKP1 and MKP2 [40]. An attractive hypothesis is that S1P5 limits ERK nuclear localization by activating nuclear phosphatases triggering ERK inactivation and subsequent cytoplasmic translocation. Alternatively, the S1P/S1P5 axis could cause the cytoplasmic retention of ERK by a yet unclear mechanism. In this regard, several spatial regulators such as β-arrestin, Sef or paxillin have been described to sequester ERK activity to the cytoplasm [27]

This study indicates that S1P5 deficiency results in a bypass of replicative senescence in primary MEFs leading to spontaneous immortalization. Two canonical pathways, p53-p21 and pRB-p16, are functionally inactivated and allow cells to escape senescence-related growth arrest [41,42] will be interesting to investigate the molecular mechanism underlying the role of S1P5 in senescence and to evaluate the role of the S1P/S1P5 pathway in oncogene- or DNA damage-induced cellular senescence.

In summary, this study revealed that S1P5, downstream ofnS1P, negatively regulates the spatiotemporal activation of ERK limiting cell proliferation and promotes the activation of FAK, controlling cell spreading and adhesion.

MATERIALS AND METHODS

Cell Culture and transfections

Mouse embryonic fibroblast (MEF) isolation and immortalization

S1P5-deficient mice have been described previously [11]. Primary MEFs isolated from wild-type ($S1P5^{+/+}$) and $S1P5^{-/-}$ embryos were a kind gift of Dr. Walzer (CIRI, Lyon, France). MEFs were maintained at 37°C in high-glucose Dulbecco's modified Eagles medium (DMEM; Gibco, LifeTechnologies, Carlsbad, CA, USA) supplemented with 10% fetal bovine serum (FBS) and penicillin/streptomycin (Sigma-Aldrich, St Louis, MO, USA) as described previously [16]. Cells from different passages were used in different experiments, as indicated in figure legends. Immortalization of primary MEFs was performed according to the 3T3 protocol [43]. For WT MEFs, when proliferation ceased, cells were maintained without passage until regrowth became apparent (P16). Cultures from passage 18 onwards were considered immortalized MEFs. Immortalized MEFs were transfected using the Amaxa Nucleofector (Lonza, Basel, Switzerland).

CHO cell lines

CHO cells were obtained from the American Type Culture Collection and grown at 37°C in a humidified atmosphere containing 5% CO_2 in Dulbecco's modified Eagles medium (4.5 g/liter glucose, GlutaMAX) supplemented with 10% heat-inactivated FBS and 100 U/ml penicillin, 100 µg/ml streptomycin. CHO cells were transfected with pcDNA-GFP-Hygro [44] or pcDNA-mS1P5-EGFP-N3 vectors, using Lipofectamine 2000 reagent (Invitrogen, Carlsbad, CA, USA) according to the manufacturer's instructions. CHO cells stably expressing mS1P5-GFP or GFP were selected in presence of 500 µg/ml hygromycin B or G418, respectively, and drug resistant clones were isolated.

Plasmids, reagents and antibodies

The synthetic *Mus musculus* sphingosine 1-phosphate receptor 5, mS1P5 (Eurofins genomics, Ebersberg, Germany), was inserted into the pEGFP-N3 vector (Clontech) using XhoI and BamHI restriction enzymes. Reagents were obtained as follows: VPC23019 from Avanti Polar Lipids (Alabaster, AL, USA), JTE-013 from Tocris (R&D Systems, Minneapolis, MN, USA); Hygromycin B, G418 and Z-VAD-

FMK from Invitrogen; S1P and FTY-720P were purchased from Enzo Life Sciences (Farmingdale, NY, USA). BrdU was obtained from Thermo Fisher Scientific (Waltham, MA, USA) and Phalloidin from Interchim (Montluçon, France). Rabbit polyclonal antibodies against p44/42 mitogen-activated protein kinase (ERK), phospho-p44/42 mitogen-activated protein kinase (phosphoERK), Akt, phospho-Akt (Ser473), FAK, phospho-FAK (Tyr575/577) were purchased from Cell Signalling Technology (Beverly, MA, USA). Mouse monoclonal antibodies against β-tubulin were from Sigma and against BrdU were from Thermo Fisher Scientific. Control (LT1017) and anti-S1P antibodies or Sphingomab™ (LT1002), a gift of Dr Sabbadini, were used as previously described [16,45].

[^{35}S] GTPγS binding assays

To prepare membrane fractions, cells were harvested in phosphate buffer saline (PBS), frozen at least overnight at -80°C, and then homogenized in ice-cold 50 mM Tris-HCl buffer, pH 7.5 using a Potter Elvehjem tissue grinder. The nuclear pellet was removed by centrifugation at 1,000 g for 15 min at 4°C. The total membrane fraction was collected after centrifugation of the supernatant at 100,000 g for 35 min at 4°C. The membrane fraction was aliquoted and stored at -80°C in 50 mM Tris-HCl, pH 7.4, and the protein concentration was determined by the Bradford method. The [^{35}S] GTPγS binding assays were performed in polypropylene tubes in a buffer consisting of 20 mM HEPES pH 7.4, 100 mM NaCl, 5 mM $MgCl_2$, 0.1% fatty acid-free BSA, and 10^{-4} M GDP. Membranes were incubated for 60 min at 30°C in the buffer supplemented with 5 µg saponin, 0.2 nM [^{35}S] GTPγS, and 1 mM of the S1PRs agonist FTY720-P. The reaction was stopped by vacuum filtration through Whatman GF/B glass filters preincubated in buffer, which were then washed three times with 4 mL of ice-cold buffer without GDP. Membrane-bound radioactivity was determined by liquid scintillation counting (Packard, GMI Trusted laboratory Solutions, Ramsey, MN, USA) after overnight extraction of the filters in 4 mL of scintillation cocktail (Ecoscint A, National Diagnostics, Fisher Scientific).

Cell proliferation and survival assays

The growth rate of immortalized MEF and CHO cells was monitored by seeding 15,000 cells and 30,000 cells per well, respectively, in triplicate in 12-well plates. At the indicated time points, the number of

viable cells was counted by trypan blue staining. For cell survival studies, 20,000 MEF were seeded in triplicate in 12-well plates and MTT assay (Sigma) was performed at the indicated time points.

BrdU incorporation

Cells were seeded and after 24 h, cell culture medium containing 10 μM BrdU was added for 4 h. Cells were washed 3 times with PBS, fixed with 3.7% paraformaldehyde and permeabilized using 0.2% Triton X-100 PBS. DNA was denaturated using 2 M HCl for 30 min, and cells were immunostained using monoclonal anti-BrdU antibodies and a rhodamine-labeled secondary antibodies. BrdU-positive cells were counted to determine the proliferation rate and the results are presented as a percentage of BrdU-positive cells.

Colony formation assays

For low-density colony formation assays, cells were seeded in 6-well plates at 500 cells/well and maintained for 10-15 days under standard culture conditions. Cells were fixed and stained with crystal violet and photographed colonies were counted using the Image J software. Results are presented as number of colonies per well.

Cell senescence assays

Senescence-associated-β-galactosidase (SA-β-Gal) activity identifies senescent cells in culture [46]. SA-β-Gal activity was measured with the senescence β-Gal kit (Cell SignallingTechnology, Beverly, MA, USA) following the manufacturer's instructions. Briefly, MEFs from different passages were fixed and SA-β-Gal activity was detected at pH 6.0. Cells with a distinctive blue color were counted and the percentage of senescent cells was determined (number SA-β-Gal positive cells/total number of cells).

Cell spreading assay

MEFs were seeded on glass coverslips and allowed to spread for 0.5, 1, 2 or 3 h at 37°C in the presence of complete media. Cells were directly fixed by adding PFA to the culture medium at a final concentration of 2% for 20 min at 37°C and stained with Phalloidin-Cy3 (1/400) for 45 min to visualize cellular outlines and with Hoechst 33342 to label DNA. Images were captured on a Nikon 90i Eclipse microscope (Nikon Instruments, NY, USA) using a 20x objective for quantifications or 40x objective for

representative images. Cell surface boundaries were outlined for n=100 randomly chosen selected cells and cell surface measurements were performed using the ImageJ software.

Cell adhesion assays

For cellular adhesion experiments, cells ($3x10^4$) were seeded in 24-well plates uncoated or coated with fibronectin (Sigma; 10 μg/ml fibronectin for 1 h at 37°C) and incubated at 37°C for the indicated times. Cells were washed 3 times with PBS to remove nonadherent cells, fixed with 3.5% formaldehyde, and stained with crystal violet after two washes. The cells were lysed and absorbance was measured at 595 nm. $S1P5^{+/+}$ cell adhesion at 30 minutes was normalized to 1, and results are presented as an adhesion fold change.

Transwell Migration Assay

Equal numbers of $S1P5^{-/-}$ and $S1P5^{+/+}$ MEFs were seeded in 8-μm pore transwell cell culture inserts (BD Biosciences, France) and complete culture medium was added to the lower compartment. Cells were allowed to migrate for 8 h at 37°C. Cells on the top side of the membrane were removed while cells that migrated to the bottom of the well were fixed and stained with crystal violet. The filters were then imaged with a Leica inverted microscope. Representative images were randomly captured for each insert and used to manually count the number of cells present. The results were expressed as relative migration normalized to wild type cells.

Immunocytochemistry

CHO cells stably expressing mS1P5-GFP or GFP alone were fixed with 4% paraformaldehyde for 10 min at room temperature and stained for DNA with DAPI prior to observation. Images were acquired on an IX73 Olympus microscope equipped with a 60X oil immersion objective (numerical aperture 1.4).

Morphological characterization of wild-type and $S1P5^{-/-}$ immortalized MEFs was performed as previously described [47]. Briefly, cells were grown on coverslips for 24 hours and stained with crystal violet. The maximal length (L) and width (W) of cells were measured using the Image J software and cell elongation was calculated as L/W.

For subcellular localization of activated ERK, MEFs were grown on coverslips in culture medium as indicated in figure legends for 24 h. Cells were washed once with PBS, fixed with 2% PFA for 20 min at 37°C, and permeabilized with 0.1% Triton X-100 PBS for 5 min. Cells were incubated with rabbit antibodies against phospho-ERK1/2 at 4°C overnight. Coverslips were washed three times with PBS and incubated with Alexa-488 anti-rabbit secondary antibodies and Phalloidin-Cy3 to stain F-actin at room temperature for 45 min. DNA was stained with Hoechst 33342. For quantification of phospho-ERK1/2 per nucleus, images were collected on a Nikon 90i Eclipse microscope using a 20x objective at the same exposure settings. Results are presented as fluorescence intensity per square micrometer.

Immunoblotting

Cells were lysed in LDS sample buffer (NuPAGE, Novex, Life Technologies), sonicated, and boiled at 96°C for 3 min. Proteins were separated on 4-20 % SDS-PAGE (Bio-Rad, Hercules, CA, USA) and transferred to polyvinylidene difluoride membrane (Immobilon-P, Millipore, Burlington, MA, USA). Membranes were blocked in TBS-T (Tris Buffered Saline with 0.1% Tween 20) containing 5% Bovine Serum Albumin (Euromedex, Souffelweyersheim, France) or 5% skim milk and incubated with primary antibodies overnight at 4°C. Membranes were washed and then incubated at room temperature with Horseradish peroxidase-conjugated secondary antibodies (Jackson ImmunoResearch, UK). After washing, detection was performed by chemiluminescence (Clarity™ Western ECL substrate, Bio-Rad). Image acquisition and quantification of immunoblots were performed with a Fusion Solo X chemiluminescence imaging system using the Evolution-Capture software (Vilber Lourmat, Marne La Vallée, France).

Data and statistical analyses

Data are presented as the means ± SEM of at least three independent experiments. Statistical analyses were performed using GraphPad Prism (version 4.0c for Macintosh, GraphPad Sofware Inc., San Diego, CA). Statistical significance for independent groups was assessed using Student's t-test. One-way analysis of variance (ANOVA) was applied to compare means. $P<0.05$ was considered a statistically significant difference.

Acknowledgments

We thank the members of Cuvillier's team for stimulating discussions. The authors are grateful to to Thierry Walzer (CIRI, Lyon, France) for providing primary MEFs from S1P5 KO mice. This work was supported by the CNRS and grants from ARTP to A.H. and from the Ministère de l'Enseignement Supérieur et de la Recherche to E.M.

Authors contribution

Conceptualization, A.B, O.C. and A.H.; methodology, F.T., E.M., C.D. and A.H.; data analysis, F.T., E.M., C.D., A.B., O.C. and A.H.; literature search, F.T., O.C. and A.H.; writing—original draft preparation, A.H.; writing—review and editing, O.C. and A.H.; supervision, O.C. and A.H.; project administration, O.C. and A.H.; funding acquisition, O.C. and A.H. All authors have read and agreed to the published version of the manuscript.

References

1. Olivera, A.; Kohama, T.; Edsall, L.; Nava, V.; Cuvillier, O.; Poulton, S.; Spiegel, S. Sphingosine kinase expression increases intracellular sphingosine-1-phosphate and promotes cell growth and survival. *J Cell Biol* 1999, *147*, 545-558.
2. Olivera, A.; Rosenfeldt, H.M.; Bektas, M.; Wang, F.; Ishii, I.; Chun, J.; Milstien, S.; Spiegel, S. Sphingosine kinase type 1 induces G12/13-mediated stress fiber formation, yet promotes growth and survival independent of G protein-coupled receptors. *J Biol Chem* 2003, *278*, 46452-46460.
3. Spiegel, S.; English, D.; Milstien, S. Sphingosine 1-phosphate signaling: providing cells with a sense of direction. *Trends Cell Biol* 2002, *12*, 236-242.
4. Brinkmann, V. Sphingosine 1-phosphate receptors in health and disease: mechanistic insights from gene deletion studies and reverse pharmacology. *Pharmacol Ther* 2007, *115*, 84-105, doi:S0163-7258(07)00083-6 [pii] 10.1016/j.pharmthera.2007.04.006.
5. Rosen, H.; Gonzalez-Cabrera, P.J.; Sanna, M.G.; Brown, S. Sphingosine 1-phosphate receptor signaling. *Annu Rev Biochem* 2009, *78*, 743-768, doi:10.1146/annurev.biochem.78.072407.103733.
6. Mendelson, K.; Evans, T.; Hla, T. Sphingosine 1-phosphate signalling. *Development* 2014, *141*, 5-9, doi:10.1242/dev.094805.
7. Maceyka, M.; Harikumar, K.B.; Milstien, S.; Spiegel, S. Sphingosine-1-phosphate signaling and its role in disease. *Trends Cell Biol* 2012, *22*, 50-60, doi:S0962-8924(11)00177-2 [pii] 10.1016/j.tcb.2011.09.003.
8. Cartier, A.; Hla, T. Sphingosine 1-phosphate: Lipid signaling in pathology and therapy. *Science* 2019, *366*, doi:10.1126/science.aar5551.
9. Talmont, F.; Hatzoglou, A.; Cuvillier, O. [Multiple sclerosis and immuno-modulators of sphingosine 1-phosphate receptors]. *Med Sci (Paris)* 2020, *36*, 243-252, doi:10.1051/medsci/2020026.
10. Graler, M.H.; Goetzl, E.J. The immunosuppressant FTY720 down-regulates sphingosine 1-phosphate G-protein-coupled receptors. *FASEB J* 2004, *18*, 551-553, doi:10.1096/fj.03-0910fje 03-0910fje [pii].
11. Jaillard, C.; Harrison, S.; Stankoff, B.; Aigrot, M.S.; Calver, A.R.; Duddy, G.; Walsh, F.S.; Pangalos, M.N.; Arimura, N.; Kaibuchi, K.; et al. Edg8/S1P5: an oligodendroglial receptor with dual function on process retraction and cell survival. *J Neurosci* 2005, *25*, 1459-1469, doi:25/6/1459 [pii] 10.1523/JNEUROSCI.4645-04.2005.
12. van Doorn, R.; Lopes Pinheiro, M.A.; Kooij, G.; Lakeman, K.; van het Hof, B.; van der Pol, S.M.; Geerts, D.; van Horssen, J.; van der Valk, P.; van der Kam, E.; et al. Sphingosine 1-phosphate receptor 5 mediates the immune quiescence of the human brain endothelial barrier. *Journal of neuroinflammation* 2012, *9*, 133, doi:10.1186/1742-2094-9-133.
13. Mayol, K.; Biajoux, V.; Marvel, J.; Balabanian, K.; Walzer, T. Sequential desensitization of CXCR4 and S1P5 controls natural killer cell trafficking. *Blood* 2011, *118*, 4863-4871, doi:10.1182/blood-2011-06-362574.
14. Chang, C.L.; Ho, M.C.; Lee, P.H.; Hsu, C.Y.; Huang, W.P.; Lee, H. S1P(5) is required for sphingosine 1-phosphate-induced autophagy in human prostate cancer PC-3 cells. *Am J Physiol Cell Physiol* 2009, *297*, C451-458, doi:10.1152/ajpcell.00586.2008.
15. Hu, W.M.; Li, L.; Jing, B.Q.; Zhao, Y.S.; Wang, C.L.; Feng, L.; Xie, Y.E. Effect of S1P5 on proliferation and migration of human esophageal cancer cells. *World J Gastroenterol* 2010, *16*, 1859-1866.
16. Andrieu, G.; Ledoux, A.; Branka, S.; Bocquet, M.; Gilhodes, J.; Walzer, T.; Kasahara, K.; Inagaki, M.; Sabbadini, R.A.; Cuvillier, O.; et al. Sphingosine 1-phosphate signaling through its receptor

S1P5 promotes chromosome segregation and mitotic progression. *Sci Signal* 2017, *10*, doi:10.1126/scisignal.aah4007.
17. Cuvillier, O.; Hatzoglou, A. Sphingosine 1-Phosphate signaling controls mitosis. *Oncotarget* 2017, *8*, 114414-114415, doi:10.18632/oncotarget.22310.
18. Todaro, G.J.; Nilausen, K.; Green, H. Growth Properties of Polyoma Virus-Induced Hamster Tumor Cells. *Cancer Res* 1963, *23*, 825-832.
19. Kilbey, A.; Blyth, K.; Wotton, S.; Terry, A.; Jenkins, A.; Bell, M.; Hanlon, L.; Cameron, E.R.; Neil, J.C. Runx2 disruption promotes immortalization and confers resistance to oncogene-induced senescence in primary murine fibroblasts. *Cancer Res* 2007, *67*, 11263-11271, doi:10.1158/0008-5472.CAN-07-3016.
20. Jodar, L.; Mercken, E.M.; Ariza, J.; Younts, C.; Gonzalez-Reyes, J.A.; Alcain, F.J.; Buron, I.; de Cabo, R.; Villalba, J.M. Genetic deletion of Nrf2 promotes immortalization and decreases life span of murine embryonic fibroblasts. *The journals of gerontology. Series A, Biological sciences and medical sciences* 2011, *66*, 247-256, doi:10.1093/gerona/glq181.
21. Price, L.S.; Leng, J.; Schwartz, M.A.; Bokoch, G.M. Activation of Rac and Cdc42 by integrins mediates cell spreading. *Mol Biol Cell* 1998, *9*, 1863-1871, doi:10.1091/mbc.9.7.1863.
22. Sieg, D.J.; Hauck, C.R.; Schlaepfer, D.D. Required role of focal adhesion kinase (FAK) for integrin-stimulated cell migration. *J Cell Sci* 1999, *112 (Pt 16)*, 2677-2691.
23. Okamoto, H.; Takuwa, N.; Gonda, K.; Okazaki, H.; Chang, K.; Yatomi, Y.; Shigematsu, H.; Takuwa, Y. EDG1 is a functional sphingosine-1-phosphate receptor that is linked via a Gi/o to multiple signaling pathways, including phospholipase C activation, Ca2+ mobilization, Ras-mitogen-activated protein kinase activation, and adenylate cyclase inhibition. *J Biol Chem* 1998, *273*, 27104-27110, doi:10.1074/jbc.273.42.27104.
24. Malek, R.L.; Toman, R.E.; Edsall, L.C.; Wong, S.; Chiu, J.; Letterle, C.A.; Van Brocklyn, J.R.; Milstien, S.; Spiegel, S.; Lee, N.H. Nrg-1 belongs to the endothelial differentiation gene family of G protein-coupled sphingosine-1-phosphate receptors. *J Biol Chem* 2001, *276*, 5692-5699, doi:10.1074/jbc.M003964200.
25. Olivera, A.; Spiegel, S. Sphingosine-1-phosphate as second messenger in cell proliferation induced by PDGF and FCS mitogens. *Nature* 1993, *365*, 557-560.
26. O'Brien, N.; Jones, S.T.; Williams, D.G.; Cunningham, H.B.; Moreno, K.; Visentin, B.; Gentile, A.; Vekich, J.; Shestowsky, W.; Hiraiwa, M.; et al. Production and characterization of monoclonal anti-sphingosine-1-phosphate antibodies. *J Lipid Res* 2009, *50*, 2245-2257, doi:M900048-JLR200 [pii]
10.1194/jlr.M900048-JLR200.
27. Ebisuya, M.; Kondoh, K.; Nishida, E. The duration, magnitude and compartmentalization of ERK MAP kinase activity: mechanisms for providing signaling specificity. *J Cell Sci* 2005, *118*, 2997-3002, doi:10.1242/jcs.02505.
28. Jenne, C.N.; Enders, A.; Rivera, R.; Watson, S.R.; Bankovich, A.J.; Pereira, J.P.; Xu, Y.; Roots, C.M.; Beilke, J.N.; Banerjee, A.; et al. T-bet-dependent S1P5 expression in NK cells promotes egress from lymph nodes and bone marrow. *The Journal of experimental medicine* 2009, *206*, 2469-2481, doi:10.1084/jem.20090525.
29. Huang, Y.L.; Chang, C.L.; Tang, C.H.; Lin, Y.C.; Ju, T.K.; Huang, W.P.; Lee, H. Extrinsic sphingosine 1-phosphate activates S1P5 and induces autophagy through generating endoplasmic reticulum stress in human prostate cancer PC-3 cells. *Cell Signal* 2014, *26*, 611-618, doi:10.1016/j.cellsig.2013.11.024.
30. Small, J.V.; Stradal, T.; Vignal, E.; Rottner, K. The lamellipodium: where motility begins. *Trends Cell Biol* 2002, *12*, 112-120, doi:10.1016/s0962-8924(01)02237-1.
31. Ilic, D.; Furuta, Y.; Kanazawa, S.; Takeda, N.; Sobue, K.; Nakatsuji, N.; Nomura, S.; Fujimoto, J.; Okada, M.; Yamamoto, T. Reduced cell motility and enhanced focal adhesion contact formation in cells from FAK-deficient mice. *Nature* 1995, *377*, 539-544, doi:10.1038/377539a0.

32. Schaller, M.D. Cellular functions of FAK kinases: insight into molecular mechanisms and novel functions. *J Cell Sci* 2010, *123*, 1007-1013, doi:10.1242/jcs.045112.
33. Lim, Y.; Lim, S.T.; Tomar, A.; Gardel, M.; Bernard-Trifilo, J.A.; Chen, X.L.; Uryu, S.A.; Canete-Soler, R.; Zhai, J.; Lin, H.; et al. PyK2 and FAK connections to p190Rho guanine nucleotide exchange factor regulate RhoA activity, focal adhesion formation, and cell motility. *J Cell Biol* 2008, *180*, 187-203, doi:10.1083/jcb.200708194.
34. Lee, O.H.; Lee, D.J.; Kim, Y.M.; Kim, Y.S.; Kwon, H.J.; Kim, K.W.; Kwon, Y.G. Sphingosine 1-phosphate stimulates tyrosine phosphorylation of focal adhesion kinase and chemotactic motility of endothelial cells via the G(i) protein-linked phospholipase C pathway. *Biochem Biophys Res Commun* 2000, *268*, 47-53, doi:10.1006/bbrc.2000.2087.
35. Miura, Y.; Yatomi, Y.; Rile, G.; Ohmori, T.; Satoh, K.; Ozaki, Y. Rho-mediated phosphorylation of focal adhesion kinase and myosin light chain in human endothelial cells stimulated with sphingosine 1-phosphate, a bioactive lysophospholipid released from activated platelets. *J Biochem* 2000, *127*, 909-914, doi:10.1093/oxfordjournals.jbchem.a022686.
36. Shikata, Y.; Birukov, K.G.; Birukova, A.A.; Verin, A.; Garcia, J.G. Involvement of site-specific FAK phosphorylation in sphingosine-1 phosphate- and thrombin-induced focal adhesion remodeling: role of Src and GIT. *FASEB J* 2003, *17*, 2240-2249, doi:10.1096/fj.03-0198com.
37. Murphy, L.O.; Blenis, J. MAPK signal specificity: the right place at the right time. *Trends Biochem Sci* 2006, *31*, 268-275, doi:10.1016/j.tibs.2006.03.009.
38. Whitehurst, A.; Cobb, M.H.; White, M.A. Stimulus-coupled spatial restriction of extracellular signal-regulated kinase 1/2 activity contributes to the specificity of signal-response pathways. *Mol Cell Biol* 2004, *24*, 10145-10150, doi:10.1128/MCB.24.23.10145-10150.2004.
39. Lidke, D.S.; Huang, F.; Post, J.N.; Rieger, B.; Wilsbacher, J.; Thomas, J.L.; Pouyssegur, J.; Jovin, T.M.; Lenormand, P. ERK nuclear translocation is dimerization-independent but controlled by the rate of phosphorylation. *J Biol Chem* 2010, *285*, 3092-3102, doi:10.1074/jbc.M109.064972.
40. Brondello, J.M.; McKenzie, F.R.; Sun, H.; Tonks, N.K.; Pouyssegur, J. Constitutive MAP kinase phosphatase (MKP-1) expression blocks G1 specific gene transcription and S-phase entry in fibroblasts. *Oncogene* 1995, *10*, 1895-1904.
41. Kim, W.Y.; Sharpless, N.E. The regulation of INK4/ARF in cancer and aging. *Cell* 2006, *127*, 265-275, doi:10.1016/j.cell.2006.10.003.
42. Papazoglu, C.; Mills, A.A. p53: at the crossroad between cancer and ageing. *J Pathol* 2007, *211*, 124-133, doi:10.1002/path.2086.
43. Rittling, S.R. Clonal nature of spontaneously immortalized 3T3 cells. *Experimental cell research* 1996, *229*, 7-13, doi:10.1006/excr.1996.0337.
44. Gomez, D.; Guedin, A.; Mergny, J.L.; Salles, B.; Riou, J.F.; Teulade-Fichou, M.P.; Calsou, P. A G-quadruplex structure within the 5'-UTR of TRF2 mRNA represses translation in human cells. *Nucleic Acids Res* 2010, *38*, 7187-7198, doi:10.1093/nar/gkq563.
45. Ader, I.; Gstalder, C.; Bouquerel, P.; Golzio, M.; Andrieu, G.; Zalvidea, S.; Richard, S.; Sabbadini, R.A.; Malavaud, B.; Cuvillier, O. Neutralizing S1P inhibits intratumoral hypoxia, induces vascular remodelling and sensitizes to chemotherapy in prostate cancer. *Oncotarget* 2015, *6*, 13803-13821.
46. Dimri, G.P.; Testori, A.; Acosta, M.; Campisi, J. Replicative senescence, aging and growth-regulatory transcription factors. *Biological signals* 1996, *5*, 154-162.
47. Hatzoglou, A.; Ader, I.; Splingard, A.; Flanders, J.; Saade, E.; Leroy, I.; Traver, S.; Aresta, S.; de Gunzburg, J. Gem Associates with Ezrin and Acts via the Rho-GAP Protein Gmip to Down-regulate the Rho Pathway. *Mol Biol Cell* 2007.

Figure Legends

Figure 1

Primary S1P5$^{-/-}$ MEFs are resistant to cellular senescence and prone to immortalization

A) Population dumplings of S1P5$^{+/+}$ and S1P5$^{-/-}$ primary MEFs over serial passaging according to 3T3 protocol. S1P5$^{+/+}$ and S1P5$^{-/-}$ MEFs were each isolated from three different embryos.

B) Wild-type and S1P5-deficient MEFs at passage 6 (P6) and passage 12 (P12), were labeled with BrdU for 3h. The incorporated BrdU was visualized by immunofluorescence. DAPI staining was used to visualize nuclei. Data represent mean +/- SEM of three different clones performed in triplicates (* p<0,0114, *** p<0,0007).

C) Colony formation capacity of S1P5$^{+/+}$ and S1P5$^{-/-}$ MEFs at passage 6 (P6). Wild type and S1P5-deficient MEFs were plated at 6 well plate and 10 days later cells were fixed and stained with crystal violet to visualize colony formation. Representative images are shown in the left panel. Right panel: quantification of colony number expressed as mean +/- SEM of three different clones performed in triplicates (*** p<0,0001).

D) S1P5$^{+/+}$ and S1P5$^{-/-}$ MEFs at passage 6 (P6) and passage 12 (P12), were stained for SA-β-Gal activity. SA-β-Gal-positive cells were counted in more than 5 fields and results represent the mean+/-SEM of three different clones performed in in triplicates (*** p<0,0001).

Figure 2

Morphological characterization of S1P5 $^{+/+}$ and S1P5 $^{-/-}$ immortalized clones

A) Phenotype of immortalized MEFs. Representative phase contrast images from low confluence cultures of S1P5$^{+/+}$ and S1P5 $^{-/-}$ cells at passage 18 after fixation and staining with crystal violet are shown in left panel. Right panel: quantification of the ratio of maximal length (L) versus cell width (W) from n=30 cells per condition of four independent experiments performed between passages 18 to 22. Each dot represents a cell (*** p<0,0001).

B) Cell area and actin organization in $S1P5^{-/-}$ cells. $S1P5^{+/+}$ and $S1P5^{-/-}$2 MEFs were plated on coverslips and 24 hours later were fixed and stained for F-Actin (Phalloidin-red) and DNA (Hoechst 33342-blue). The left panel shows representative images. Scale bar, 20 μm. The right panel shows the quantification of the cell area (in square micrometers) based on F-Actin staining. The mean surface area was calculated using ImageJ software. The data are represented in a dot blot, where each point represents one cell and the black lines indicate mean+/-SEM (***P < 0.0001; $S1P5^{+/+}$, 2612 ± 255.2 n=41; $S1P5^{-/-}$ 1467 ± 146.7, n=50).

Figure 3

Impaired adhesion, spreading and migration in $S1P5^{-/-}$ cells

A & B) $S1P5^{+/+}$ and $S1P5^{-/-}$2 MEFs were plated on non-coated (A) or fibronectin-coated (B) 24-well plates and incubated for 0.5, 1, and 2 h. Cells were washed and the adherent cells were stained with crystal violet, and the staining intensity was quantified by spectrophotometry at 560 nm. The results represent fold cell adhesion (of wild-type cells) and are mean+/-SEM of three independent experiments (**p<0,0083, *p<0,0149, **p<0,0073, *p<0,0226).

C) Cell spreading and actin organization in $S1P5^{-/-}$ cells. $S1P5^{+/+}$ and $S1P5^{-/-}$2 MEFs were plated on coverslips for the indicated times, fixed and stained for F-Actin (Phalloidin-red) and DNA (Hoechst 33342-blue). The upper panel shows representative images. Scale bar, 20 μm. The lower panel shows the quantification of the cell area (in square micrometers) based on F-Actin staining. The mean surface area from 100 individual cells was calculated using ImageJ software. The data are shown as dot blot, where each point represents one cell and the black lines indicate mean+/-SEM (***P < 0.0001).

D) Equal numbers of $S1P5^{+/+}$ and $S1P5^{-/-}$ MEF cells were seeded on the top of 8-μm pore Transwell cell culture inserts and incubated for 8 h. The cells migrated to the bottom of the well were fixed and stained with crystal violet. Left panel shows representative images and right panel the relative migration (% of control cells). The mean+/- SEM from four experiments is shown (***, p<0.0001).

E) Impaired FAK phosphorylation in $S1P5^{-/-}$ MEF cells. $S1P5^{+/+}$ and $S1P5^{-/-}$ cells were serum-starved for 4h and then treated with S1P (1μM) for different times as indicated. Total cell extracts were analyzed

by SDS/PAGE with antibodies against phosphorylated FAK, FAK and tubulin. Right panel shows SDS/PAGE of $S1P5^{+/+}$ and $S1P5^{-/-}$ cells cultured in medium containing 10% FCS. After 24 hours cells were lysed and total cell extracts were analyzed by SDS/PAGE with antibodies against phosphorylated FAK, FAK and tubulin.

Figure 4

Growth properties of immortalized S1P5-deficient cells

A) $S1P5^{+/+}$ and $S1P5^{-/-}$ cells were plated at equal cell number and the cell number was daily counted over a period of 4 days. Results are representative from four independent experiments performed in triplicates from MEFs at passages 18 to 22.

B) Cell survival of $S1P5^{+/+}$ and $S1P5^{-/-}$ MEFs (passages 18-22) was assessed with MTT assay at the indicated times after seeding. Results are representative from three independent experiments performed in triplicates.

C) Colony formation capacity of the immortalized $S1P5^{+/+}$ and $S1P5^{-/-}$ MEFs between passages 18-22. Low number of cells were plated and allowed to grow for 10 days. Cells were then fixed and stained with crystal violet to visualize colony formation. Graph shows the mean colony number +/- SEM of three independent experiments performed in triplicates (*p<0,0357, **p<0,0017).

D) Cell death/viability was evaluated by trypan blue staining. $S1P5^{+/+}$ and $S1P5^{-/-}$ cells were plated at equal cell number and the number of trypan blue-positive cells was counted at the indicated time points. Results are mean+/- SEM of three independent experiments performed in triplicates. (ns; Student's test).

E) Equal number of $S1P5^{+/+}$, $S1P5^{+/+}$ clone 2 ($S1P5^{+/+}2$) and $S1P5^{-/-}2$ cells were plated and the cell number was counted 72 hours later. Results represent mean of relative cell number +/- SEM of three independent experiments performed in triplicates (***p<0,0007, ns p=0,6279).

F) S1P5 rescues the $S1P5^{-/-}$ phenotype. Immortalized MEF $S1P5^{-/-}$ clone 1 and clone 2 were transiently transfected with empty vector (GFP) or a vector containing mS1P5-GFP. The total cell number was

evaluated at different post transfection times. Results represent mean of relative cell number +/- SEM of three independent experiments performed in triplicates (**p< 0,0058, **p<0,0099, **p<0,0079, ns p=0,1879).

Figure 5

S1P5 induces growth arrest / S1P5 inhibits cell growth

A) Representative images showing CHO cells stably expressing GFP or mS1P5-GFP and stained for DNA with DAPI. Scale bar, 10 μm. Right panel shows GFP and mS1P5-GFP levels in CHO cells analyzed by Western blot using antibodies against GFP.

B) Pharmacological characterization of mS1P5R-GFP. Agonist and antagonist stimulation of CHO cells ectopically expressing mS1P5-GFP or GFP alone. Membrane fractions were isolated and stimulated with increased concentrations of S1P or FTY-720P. The graph is representative of two independent experiments each comprising duplicate determinations.

C) Growth properties of CHO cells stably expressing mS1P5R-GFP or GFP. CHO mS1P5-GFP or CHO GFP cells were plated at equal cell number and the cell number was daily counted over a period of 4 days. Growth curve is mean +/- SEM of pool results from three independent experiments performed in triplicates (**p<0,0021, *p<0,0134, *p<0,0157).

Figure 6

Extracellular S1P induces growth arrest via S1P5 in CHO cells / S1P5-induced growth inhibition is S1P5 dependent

A) CHO cells expressing mS1P5-GFP or GFP alone were plated at 20000 cells/well in 12 well plates. 16h later cells were non-treated (NT) or treated with Z-VAD (10μM), vehicle (DMSO), or FTY720-P (1μM) and the cell number was counted 48 hours post treatment. Results are mean +/- SEM from three independent experiments performed in triplicates (***p<0,0007, **p<0,0022, **p<0,0045, ns p=0,4818).

C) mS1P5-GFP or GFP expressing CHO cells were plated as in A and treated with control antibodies (α-Ctl) or antibodies against S1P (α-S1P). The cell number was counted 48 hours post treatment. Results are mean +/- SEM from four independent experiments performed in triplicates *p<0,0232, ns p=0,8298).

B) CHO cells expressing mS1P5-GFP or GFP alone were plated as in A. 16h later cells were washed and treated in DMEM delipidated FBS (csFBS) for 24h in absence, or in presence of S1P (1μM) or S1P and α-S1P. Cells cultured in medium containing 10%FCS were also counted (FCS). Results show cell number 48 hours post treatment and are mean +/- SEM from at least three independent experiments performed in triplicates (***p<0.0001, ns p=0,6309, *p<0,0192, ns p=0,6870).

Figure 7

Knockdown of S1P5 promotes cells growth in S1P dependent manner

A) $S1P5^{+/+}$ and $S1P5^{-/-}$ cells were plated at 20000 cells/well and 16h later cells were treated with vehicle (DMSO), Z-VAD (10μM), FTY720-P (1μM) or VPC23019 (10μM) +JTE-013 (10μM). Results show relative cell number expressed as % of control non treated cells +/- SEM from more than three independent experiments performed in triplicates (***p<0.0004, **p<0,0085, ***p<0.0006, ns p=0,8656, **p<0,0049, *p<0,0217).

B) $S1P5^{+/+}$ and $S1P5^{-/-}$ cells cultured as in A and were either cultured in DMEM containing delipidated FBS (csFBS) or in complete medium containing FBS in presence of control antibodies (α-Ctl) or antibodies against S1P (α-S1P). The cell number was counted 48 hours post treatment. Results show relative cell number expressed as % of control non-treated cells +/- SEM from three independent experiments performed in triplicates (**p<0.0010, ns p=0,4685, *p<0,0304, ns p=0,7922, **p <0,0016).

Figure 8

S1P5 reduces nuclear P-ERK localization

A) S1P5$^{+/+}$ and S1P5 $^{-/-}$ cells were cultured in medium containing 10% FCS during 24 hours. Total cell extracts were analyzed by SDS/PAGE with antibodies against the indicated proteins.

B) S1P5$^{+/+}$ and S1P5 $^{-/-}$ MEFs were cultured as in A, fixed and stained for phospho-ERK (α-ERK-green), DNA (Hoechst 33342-blue) and actin (phalloidin-red). Scale bar, 20 µm.

C) Quantification of nuclear phospho-ERK staining based on anti-ERK and Hoechst 33342 staining. Images were taken with 20x objectif and the same exposure settings were used for all fluorescence quantifications. Results are expressed as fluorescence intensity per square micrometer (***P < 0.0001; S1P5$^{+/+}$, 423.3 ± 33.30, n=52; S1P5$^{-/-}$ 603.6 ± 30.77, n=61).

Figure S1

Actin organization and FA in S1P5$^{-/-}$ MEFs

A. Representative images of S1P5$^{+/+}$ and S1P5 $^{-/-}$ MEFs cultured in medium containing 10% FCS. Cells were fixed 24 hours post platting and stained for F-Actin (Phalloidin-red) and DNA (Hoechst 33342-blue). Scale bar, 20 µm.

B. Representative images of S1P5$^{+/+}$ and S1P5 $^{-/-}$ MEFs cultured as in A and stained for F-Actin (Phalloidin-red), vinculin (a-vin-green) and DNA (Hoechst 33342-blue). Scale bar, 20 µm.

Figure S2

FAK phosphorylation is decreased in S1P5-/- MEFs

S1P5$^{+/+}$ and S1P5 $^{-/-}$ MEFs were cultured in medium containing 10% FCS during 24h and the total cell extracts were analyzed by SDS/PAGE with antibodies against phosphorylated FAK, FAK and tubulin. Data represent the quantification of relative P-FAK/FAK levels of 3 independent experiments (mean+/-SEM).

Figure 1

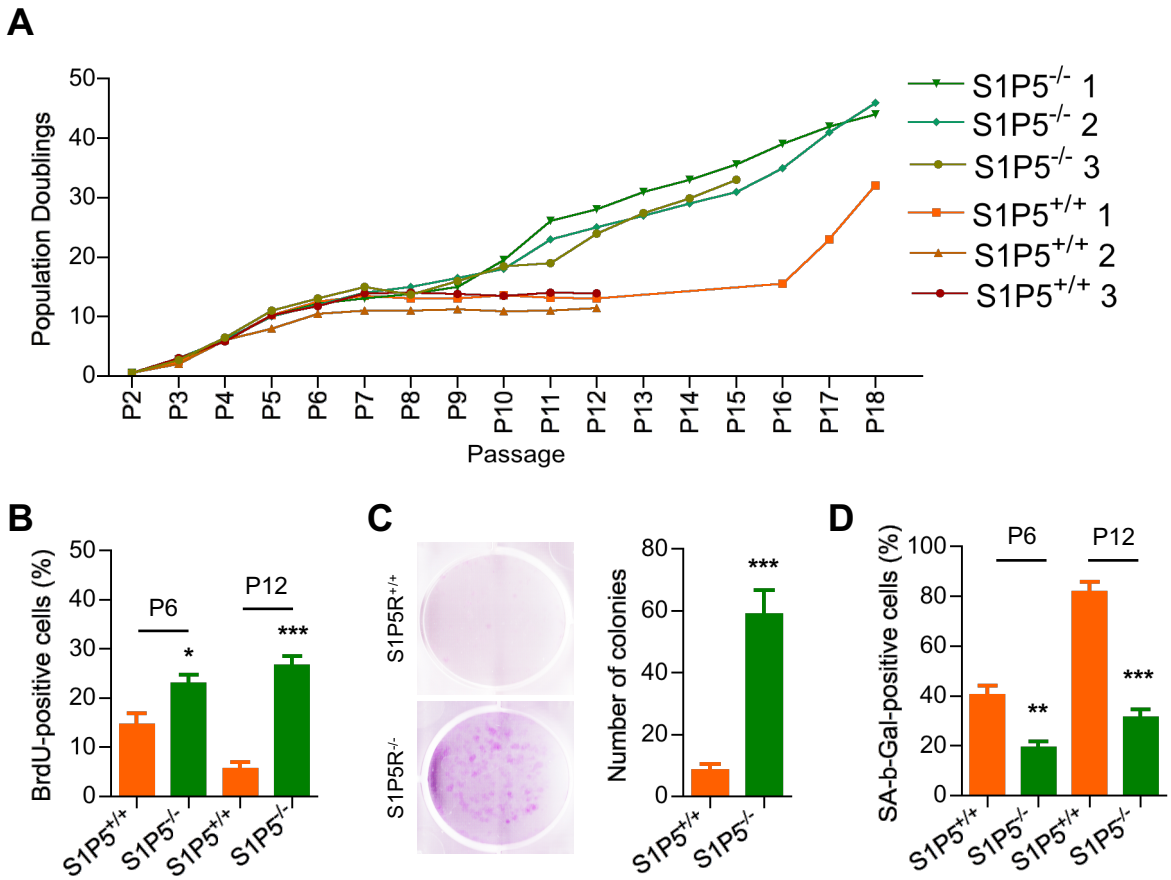
A
Population Doublings
Passage
S1P5-/- 1
S1P5-/- 2
S1P5-/- 3
S1P5+/+ 1
S1P5+/+ 2
S1P5+/+ 3
B
BrdU-positive cells (%)
P6
P12
C
S1P5R+/+
S1P5R-/-
Number of colonies
D
SA-b-Gal-positive cells (%)

Figure 2

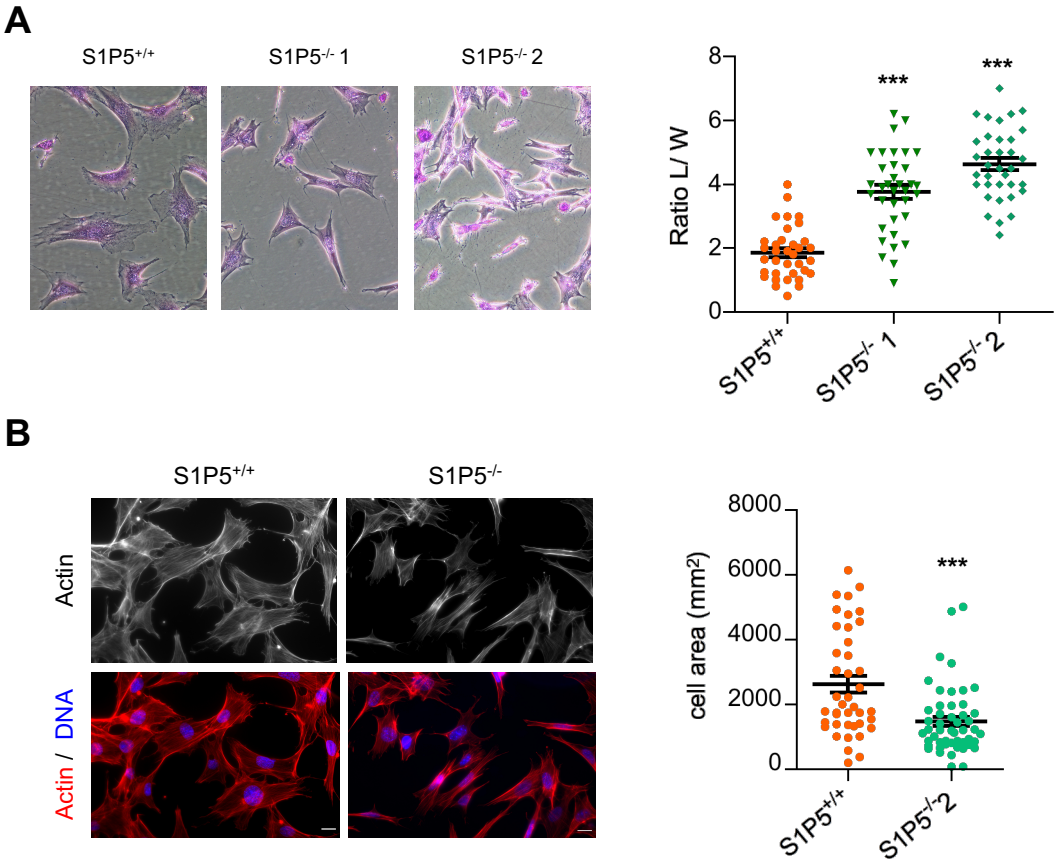
A
S1P5+/+
S1P5-/- 1
S1P5-/- 2
Ratio L/ W
8
6
4
2
0
***
***
S1P5+/+
S1P5-/- 1
S1P5-/- 2
B
S1P5+/+
S1P5-/-
Actin
Actin / DNA
cell area (mm2)
8000
6000
4000
2000
0
***
S1P5+/+
S1P5-/-2

Figure 3

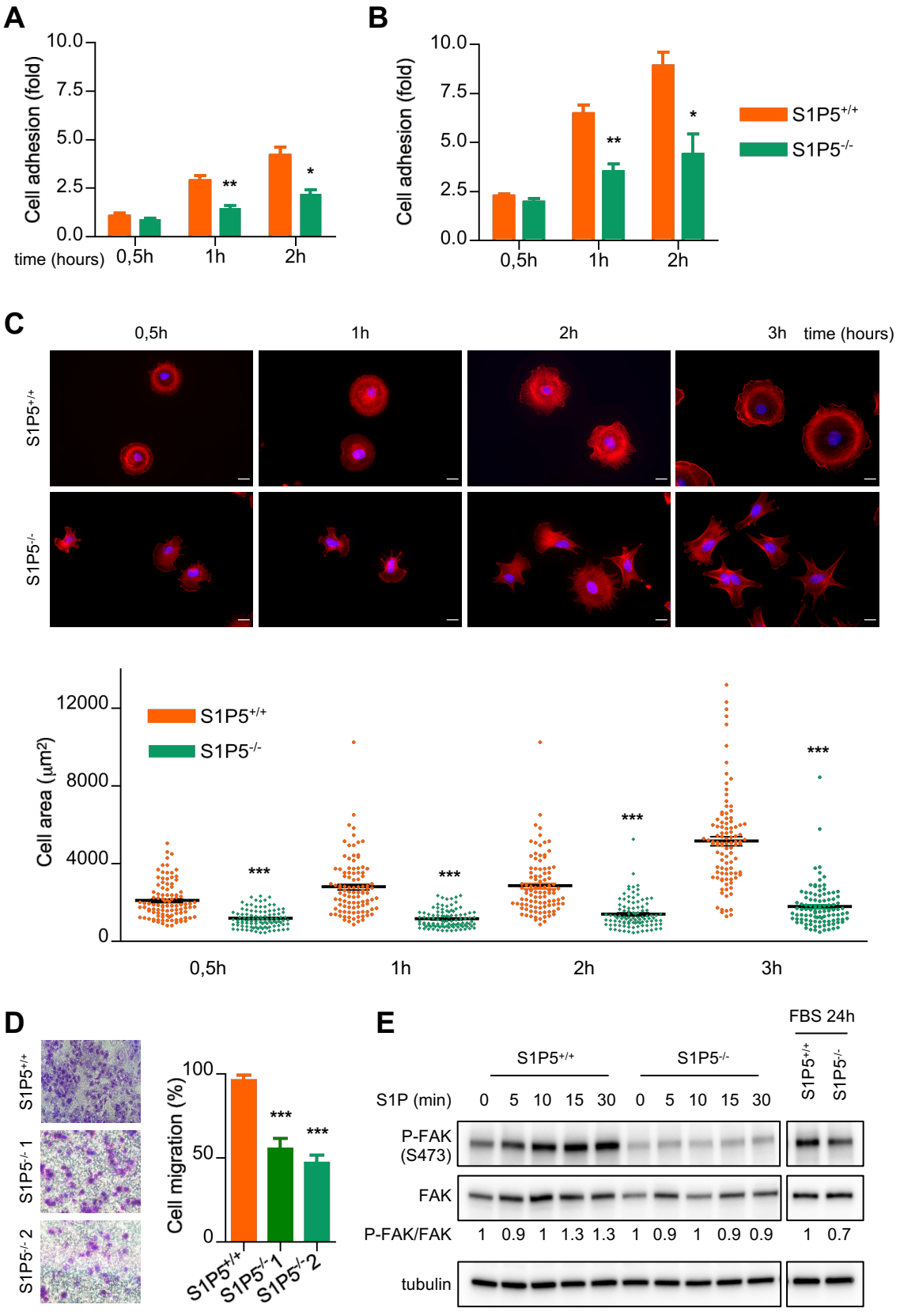
A
Cell adhesion (fold)
10.0
7.5
5.0
2.5
0.0
time (hours)
0,5h
1h
2h
**
*
B
Cell adhesion (fold)
S1P5+/+
S1P5-/-
C
0,5h
1h
2h
3h
time (hours)
S1P5+/+
S1P5-/-
Cell area (µm2)
12000
8000
4000
0
***
D
S1P5+/+
S1P5-/- 1
S1P5-/- 2
Cell migration (%)
100
50
0
E
FBS 24h
S1P (min)
0 5 10 15 30 0 5 10 15 30
P-FAK (S473)
FAK
P-FAK/FAK
1 0.9 1 1.3 1.3 1 0.9 1 0.9 0.9 1 0.7
tubulin

Figure 4

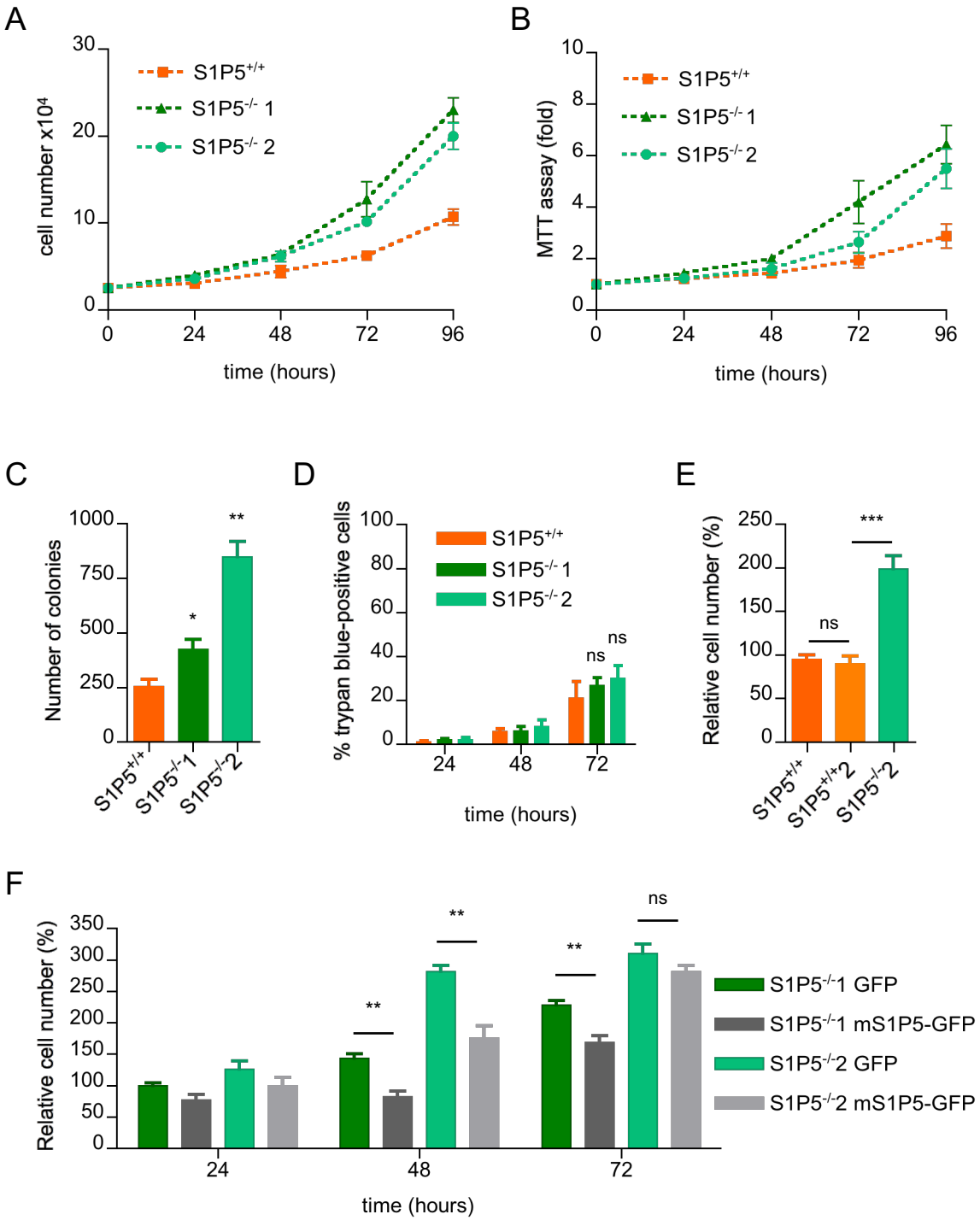
A
cell number x10⁴
30
20
10
0
S1P5+/+
S1P5-/- 1
S1P5-/- 2
0
24
48
72
96
time (hours)
B
MTT assay (fold)
10
8
6
4
2
0
S1P5+/+
S1P5-/- 1
S1P5-/- 2
0
24
48
72
96
time (hours)
C
Number of colonies
1000
750
500
250
0
**
*
S1P5+/+
S1P5-/-1
S1P5-/-2
D
% trypan blue-positive cells
100
80
60
40
20
0
S1P5+/+
S1P5-/- 1
S1P5-/- 2
ns
ns
24
48
72
time (hours)
E
Relative cell number (%)
250
200
150
100
50
0
***
ns
S1P5+/+
S1P5+/+2
S1P5-/-2
F
Relative cell number (%)
350
300
250
200
150
100
50
0
**
**
**
ns
24
48
72
time (hours)
S1P5-/-1 GFP
S1P5-/-1 mS1P5-GFP
S1P5-/-2 GFP
S1P5-/-2 mS1P5-GFP

Figure 5

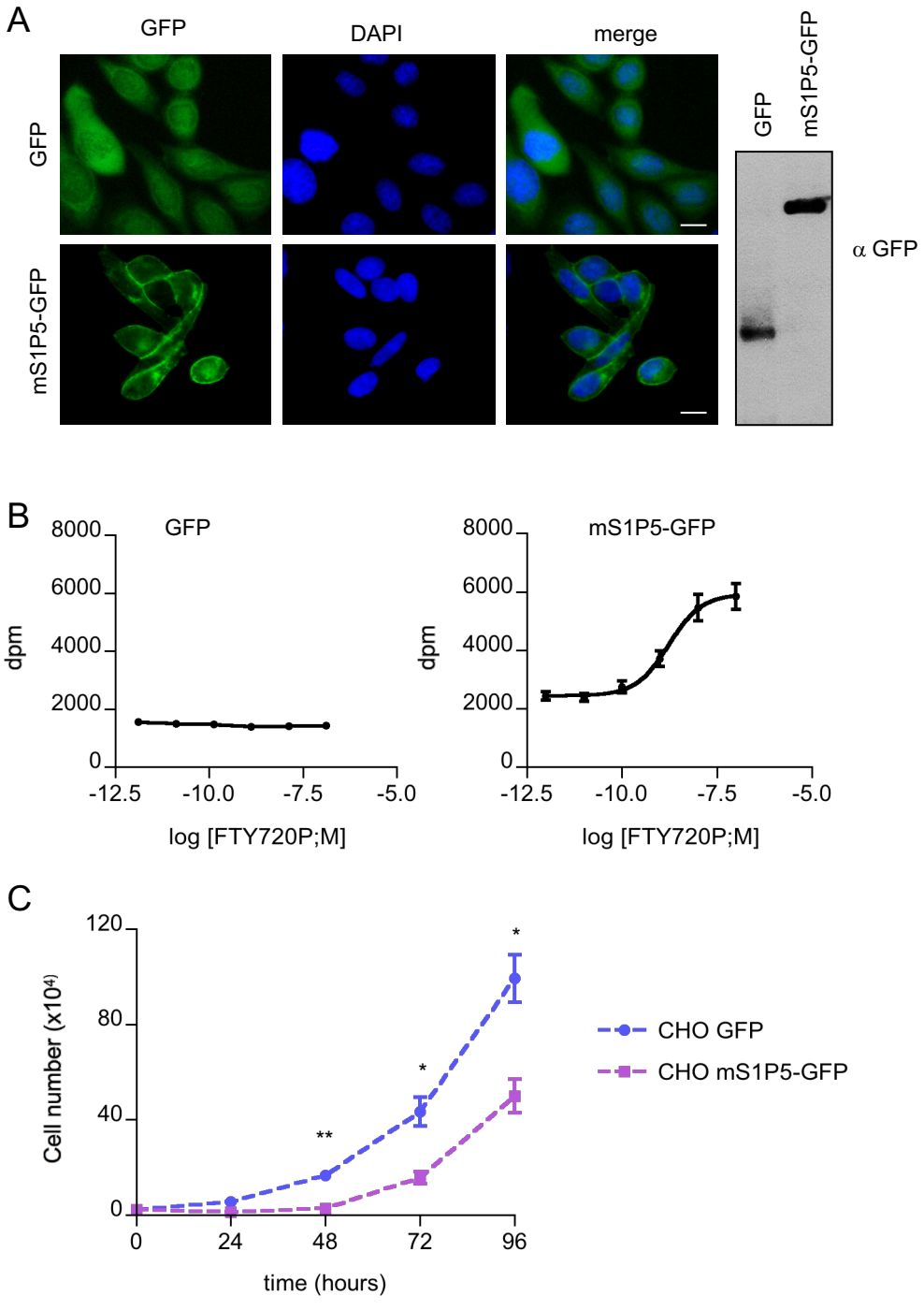
A
GFP
DAPI
merge
GFP
mS1P5-GFP
GFP
mS1P5-GFP
α GFP
B
GFP
mS1P5-GFP
dpm
8000
6000
4000
2000
0
-12.5
-10.0
-7.5
-5.0
log [FTY720P;M]
C
Cell number (x10⁴)
120
80
40
0
0
24
48
72
96
time (hours)
*
*
**
CHO GFP
CHO mS1P5-GFP

Figure 6

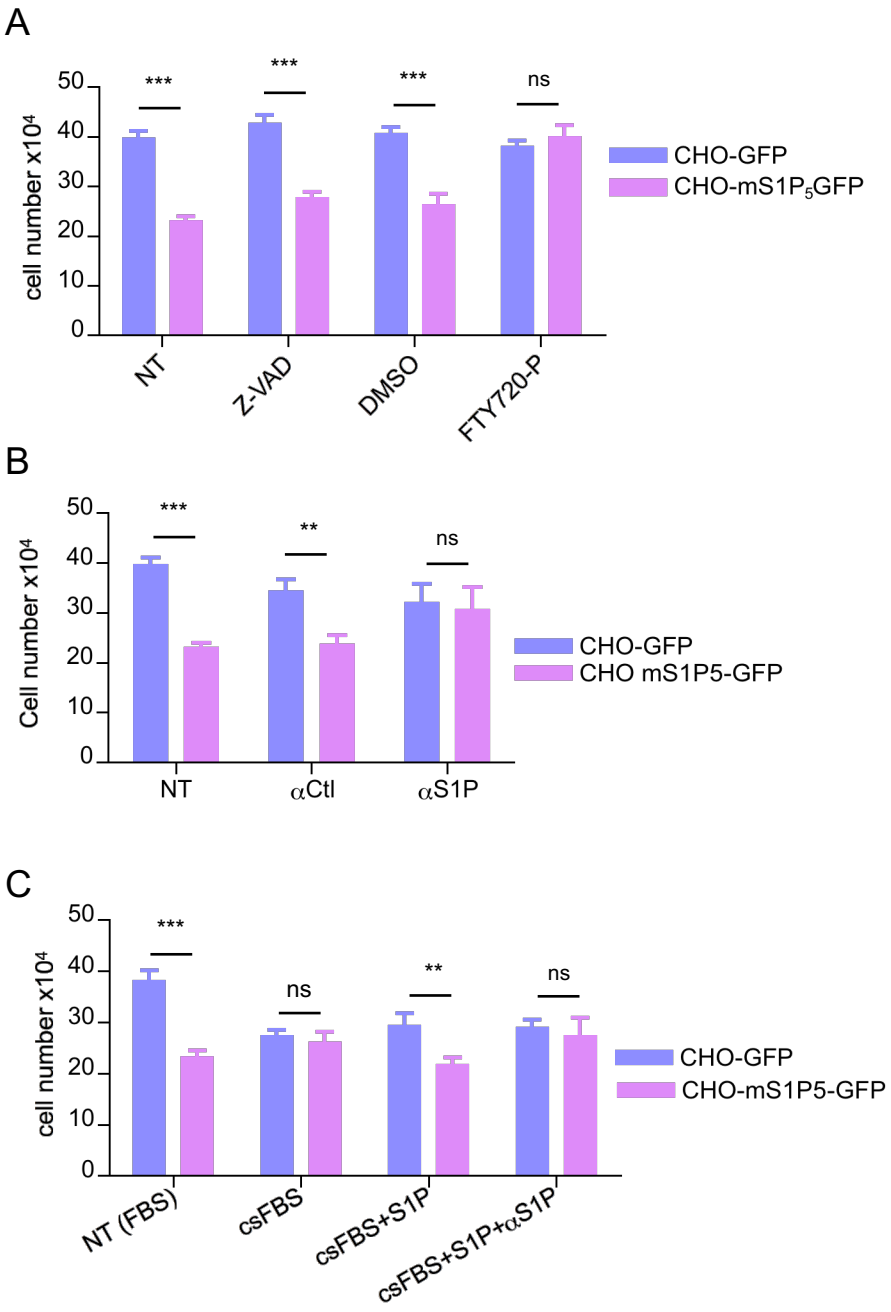
A
cell number x10⁴
50
40
30
20
10
0
***
***
***
ns
NT
Z-VAD
DMSO
FTY720-P
CHO-GFP
CHO-mS1P5GFP
B
Cell number x10⁴
50
40
30
20
10
0
***
**
ns
NT
αCtl
αS1P
CHO-GFP
CHO mS1P5-GFP
C
cell number x10⁴
50
40
30
20
10
0
***
ns
**
ns
NT (FBS)
csFBS
csFBS+S1P
csFBS+S1P+αS1P
CHO-GFP
CHO-mS1P5-GFP

Figure 7

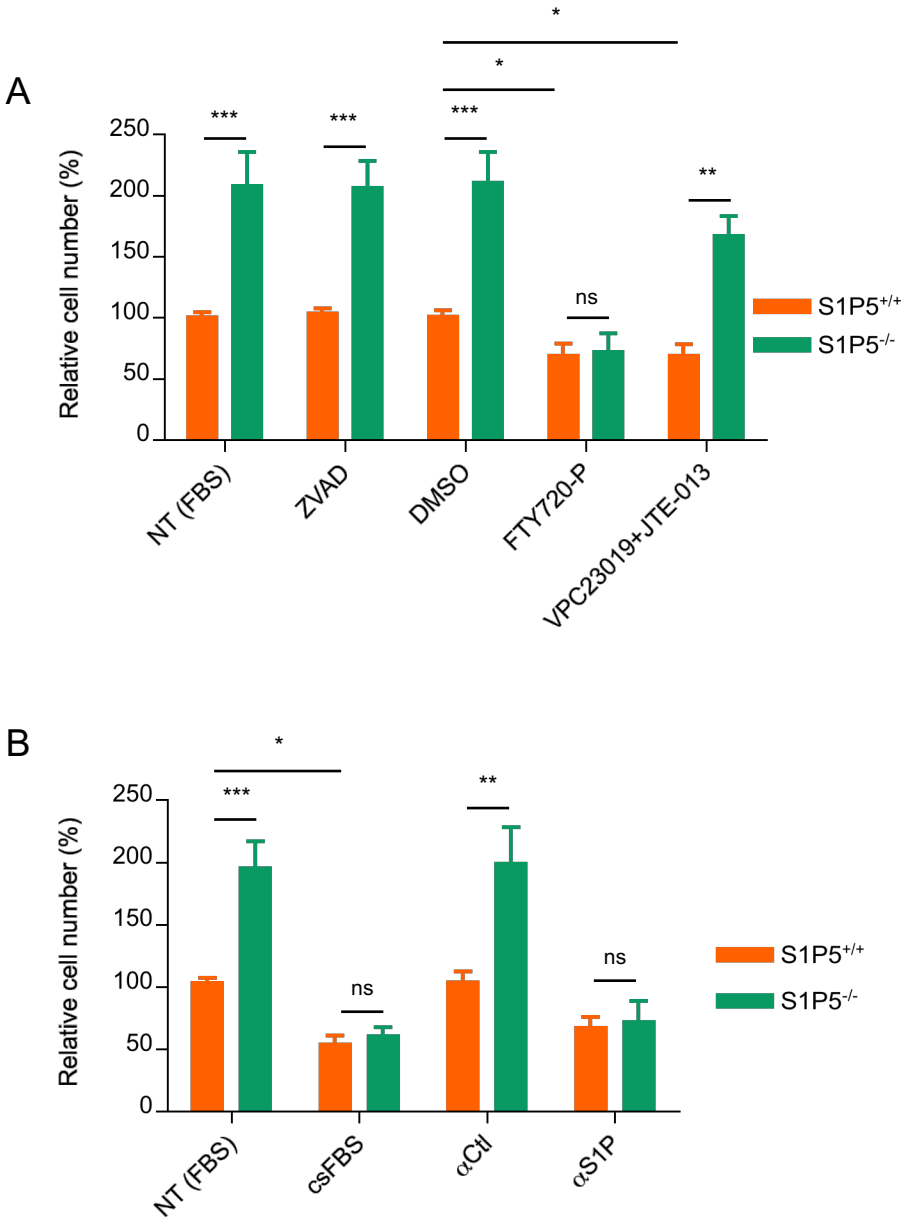
A
Relative cell number (%)
250
200
150
100
50
0
***
***
***
*
*
**
ns
NT (FBS)
ZVAD
DMSO
FTY720-P
VPC23019+JTE-013
S1P5+/+
S1P5-/-
B
Relative cell number (%)
250
200
150
100
50
0
*
***
ns
**
ns
NT (FBS)
csFBS
αCtl
αS1P
S1P5+/+
S1P5-/-

Figure 8

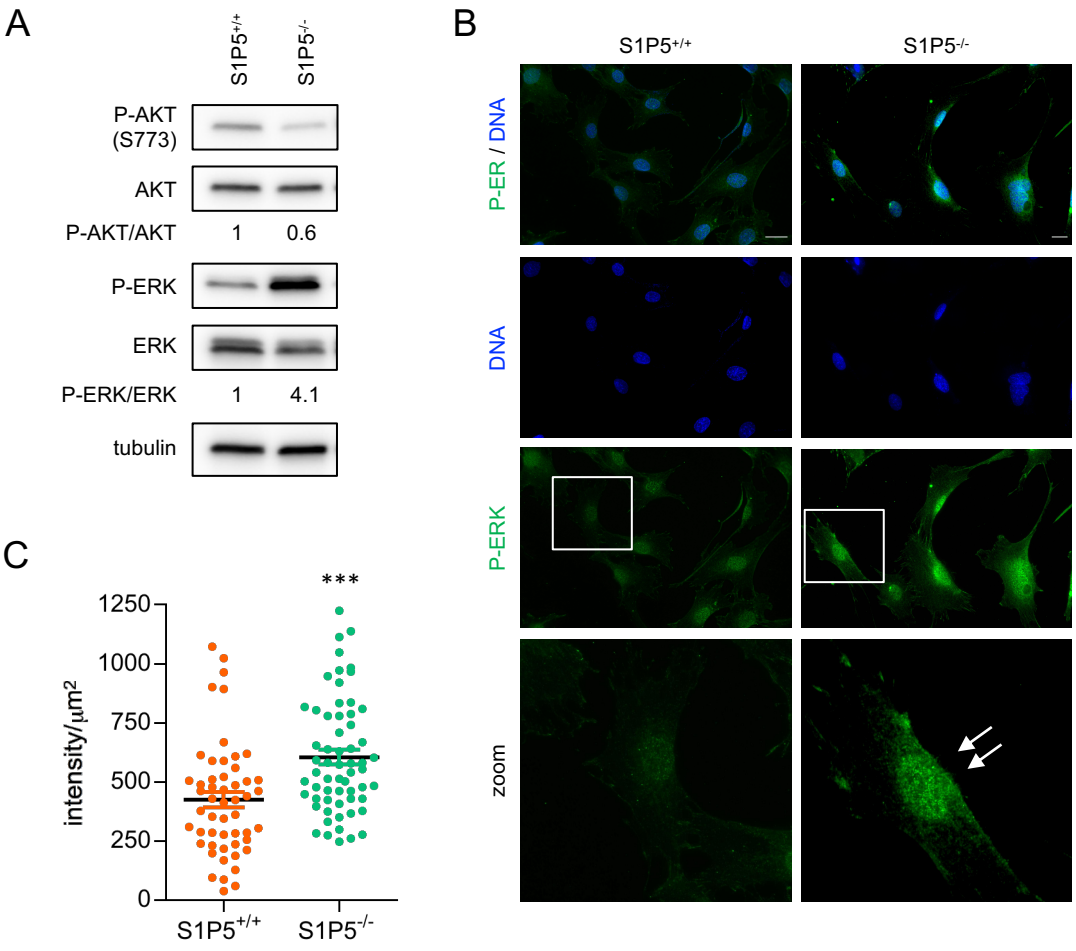
A
S1P5+/+
S1P5-/-
P-AKT (S773)
AKT
P-AKT/AKT
1
0.6
P-ERK
ERK
P-ERK/ERK
1
4.1
tubulin
B
S1P5+/+
S1P5-/-
P-ER / DNA
DNA
P-ERK
zoom
C
***
intensity/µm2
1250
1000
750
500
250
0
S1P5+/+
S1P5-/-

Figure S1

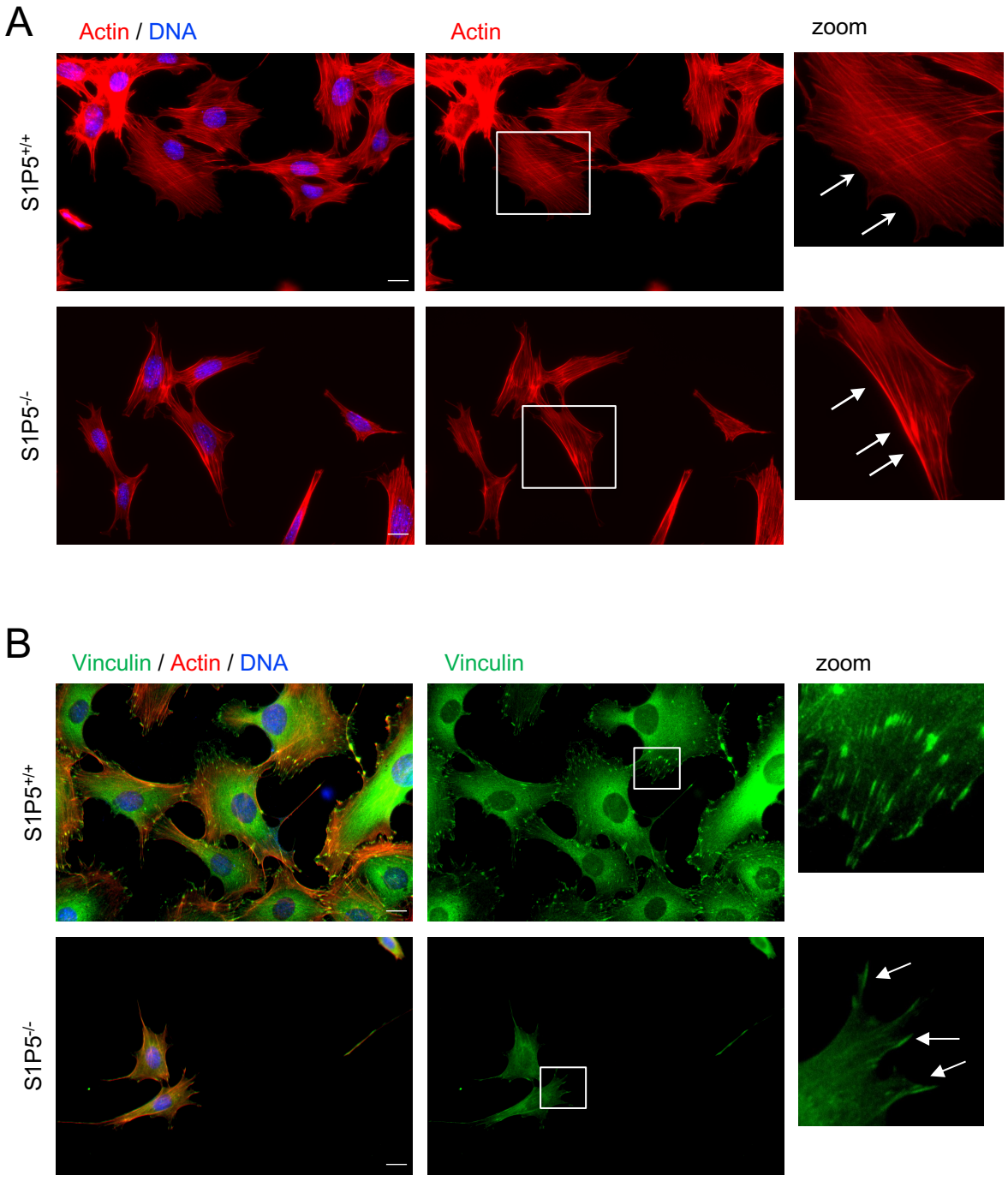
A
Actin / DNA
Actin
zoom
S1P5+/+
S1P5-/-
B
Vinculin / Actin / DNA
Vinculin
zoom
S1P5+/+
S1P5-/-

Figure S2